polymer papers

Quantitative evaluation of the Gibbs theory of the glass transition

R. P. Kusy and A. R. Greenberg*
Dental Research Center, University of North Carolina, Chapel Hill, NC 27514, USA
(*Received* 3 *November* 1982; *revised* 5 *August* 1983)

The utility of a reduced parametric plot of glass transition ($T_g/T_{g\infty}$) *versus* the reciprocal degree of polymerization ($10^3/\bar{P}$) is reviewed and illustrated for the case of the Gibbs theory of the glass transition. These results show that the number of lattice sites occupied per mer (n) affects T_g more than variations in the fractional free volume at T_g (V_0). Traditionally a variation of the Gibbs theory ($n=1$) has been used to explain the $\bar{P}$ dependence of T_g for poly(methyl methacrylate) (PMMA). However, statistical analyses of all available PMMA data sets show that there is an interrelation between n and V_0 at the 0.05 level such that many acceptable solutions occur, one of which is at $V_0=0.025$ and $n=1.25$. Therefore, a unique solution may not be obtained unless a free volume is either (1) assumed as Gibbs and others had routinely done, or, more properly, (2) calculated from the PVT equation of state. In the latter case, however, knowledge of the ratio of hole energy to flex energy (r) is required. With only subjective evaluations previously available, the statistical methodology is presented as an alternative, objective approach to compare T_g data with theory.

(Keywords: Glass transition; poly(methyl methacrylate); Gibbs theory; free volume; hole energy; flex energy)

INTRODUCTION

In describing their refractomeric technique used to measure the glass transition in poly(methyl methacrylate) (PMMA), Beevers and White (B & W)[1] reviewed the experimental work of, among others, Flory, Fox, Mandelkern, and Tobolsky. Subsequently, B & W selected three theories to describe their results: the straight line approach which relates the reciprocal of the degree of polymerization $(\bar{P})^{-1}$ to the glass transition (T_g) (ref. 2), and the statistical mechanical theories of Gibbs (G)[3] and Gibbs–DiMarzio (G–DM)[4]. Of these, the G theory was acknowledged to yield the best agreement, i.e.:

$$\frac{2\beta \exp\beta}{1+2\exp\beta} - \ln[1+2\exp\beta] = -\frac{\bar{x}}{\bar{x}-2}\left[\frac{V_0 \ln V_0}{1-V_0} - \frac{\ln 2\bar{x}}{\bar{x}-2} + \frac{\bar{x}-1}{\bar{x}-2}\right] \quad (1)$$

in which β equalled the flex energy divided by the product of Boltzman's constant and $T_g(=-\varepsilon/kT_g)$, V_0 was the fractional free volume at T_g, and $\bar{x}$ (the number average of chain atom segments**) was equated to $\bar{P}$. On this basis $\varepsilon=0.98$ Kcal mol^{-1} segment, $V_0=0.025$, and $T_{g\infty}=390$ K. Later work by Thompson[5] on stereoregular PMMA's, by Pratt[6] on irradiated acrylic, and by Kim *et al.*[7] on the dynamic mechanical properties of PMMA and its copolymers simply described T_g in terms of reciprocal chain length.

In more recent work, the G theory has been employed to describe the T_g dependence on irradiated fractions[8] and polymer blends[9]. In the first case, exposure to as much as 500 Mrad of ^{137}Cs γ-rays reduced $\bar{P}$ from 5900 to 12. For $V_0=0.025$, ε equalled 0.97 ($T_{g\infty}=385$ K) or 1.00 ($T_{g\infty}=395$ K) Kcal mol^{-1} segments depending upon the specific convention of T_g adopted. In the second case, polymer blends were prepared from three feedstocks having $P=39$, 321, and 1220. For all three binary systems, $\varepsilon=0.99$–1.00 Kcal mol^{-1} segments ($T_{g\infty}=395.1$–399.1 K) when once again $V_0=0.025$. In both these cases only one lattice site was occupied per mer, i.e. $\bar{x}=n\bar{P}$ in which $n=1$.

In the most recent effort the influence of V_0, the inter-/intramolecular energy ratio (r), and the chain segment density (n) were evaluated for the G–DM theory[10]. Using reduced variables plots, a family of curves was generated, the slopes of which decreased with increasing n as either V_0 or r was fixed at 0.015, 0.030, and 0.045 or 0.8, 1.0, and 1.2, respectively. Of the four polymers evaluated, PMMA was bracketed by $n=1$, $V_0=0.030$, and by $n=2$, $V_0=0.030$ ($r=0.7$–1.1). The present work not only demonstrates the parametric variations of the G theory but also evaluates the overall fit of PMMA data via statistical analysis techniques.

THEORETICAL CONSIDERATIONS

Figure 1 outlines the methods and rationale used in the construction of the reduced T_g plots. If T_g is plotted against both the reciprocal of the number average molecular weight ($\bar{M}_n$) and ε, a unique surface is generated for each value of V_0. Such a solution set may be computed for each different polymer having mer molecular weights, $M_0=A$,

* Present address: Department of Mechanical Engineering, University of Colorado, Boulder, CO 80309, USA.

** In B & W's original work, this equation was actually used to determine curve 3 of Figure 3, although the stated expression substituted $\bar{P}$ for $\bar{P}-2$ in the last two terms enclosed by brackets. For the case of PMMA such an assignment would have reduced T_g by 2, 17, and 88 K for a $\bar{P}$ of 1000, 100, and 10, respectively.

0032-3861/84/050600-09$03.00

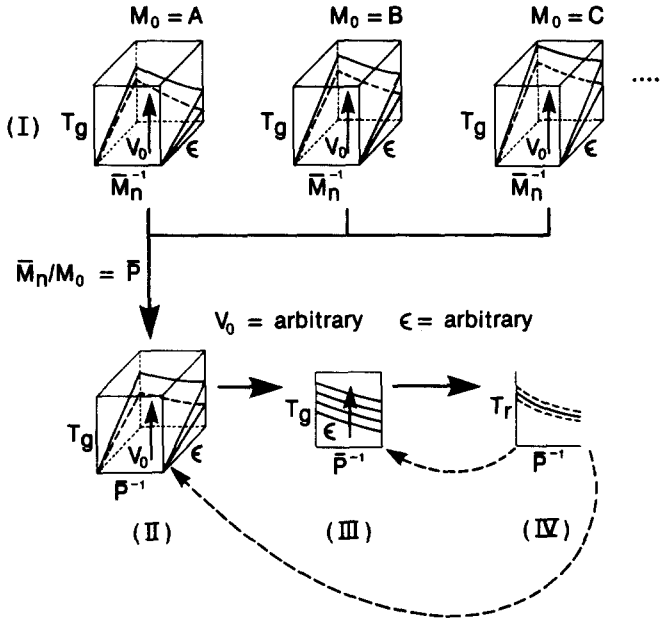

Figure 1 Construction of a reduced T_g plot ($T_r = T_g/T_{g\infty}$; *cf.* text for details)

B, C, ..., in which A ≠ B ≠ C ... (*cf.* Part I). By capitalizing on the fact that $M_n/M_0 = P$, all polymers may be reduced to a mer molecular weight basis, i.e. to a single three-dimensional diagram (*cf.* Part II). The actual diagrams have been illustrated in Figure 2 of ref. 11 for both the G and G–DM theories. Over the extensive range of parameters investigated, i.e. $\bar{P} = 10$–∞, $\varepsilon = 0$–2.5 Kcal mol^{-1} segment, and $V_0 = 0.015$–0.045, T_g was most sensitive to changes in ε. Consequently, if a constant V_0 surface were chosen arbitrarily and ε values were restricted to discrete intervals, a two-dimensional plot would result (*cf.* Part III). Knowing that the reduced parameter, $T_r = T_g/T_{g\infty}$, is directly proportional to the ε ratio and assuming that ε is constant for any $\bar{P}$, T_r is an inverse function of the β's alone (*cf.* solid line, Part IV). This functionality is true for any arbitrary value of ε (*cf.* the dashed feedback loop between Parts III and IV) and, indeed, only broadens slightly when V_0 is extended over a sensible range (*cf.* the dashed feedback loop between Parts II and IV and the dashed envelope about the solid line in Part IV). The single curvilinear bands have been shown for both statistical mechanical theories with the constraints that the sublattices of co-ordination number $z = 4$, $z' = 4$, $\alpha = \infty$, and $\bar{x} = 2\bar{P}$ for the G–DM theory*, and that $z = 4$, $z' = \infty$, and $\bar{x} = 2\bar{P}$ for the G theory (*cf.* curves 1 and 2, Figure 1, ref. 11).

The constraint that $n = 2$ in $\bar{x} = n\bar{P}$ is based on the tenuous assumption that, for vinyl polymers, each backbone carbon atom and its attendant side groups occupies only one lattice site. If the size of a methylene group is arbitrarily taken to define the dimensions of a lattice site[17], then the presumption that $n = 2$ is likely to be in error more often than not. For example, the number of lattice sites occupied per mer, i.e. 'beads', has been calculated for four well-documented polymers, PMMA, PS, PVC, and PαMS, and the results indicate that n equals 5.9, 6.1, 3.0, and 7.4, respectively (*cf.* Table 2, ref. 18). While PMMA, PS, and PαMS have similar values, T_r *versus* $\bar{P}^{-1}$ measurements indicate that the n's are not comparable; on the contrary, PαMS is much more P^{-1} dependent. Another approach can be taken whereby the number of flexible bonds per monomer, i.e. 'flexes', is assumed to be proportional to n. For this case the corresponding values that have been suggested are 3–4, 2, 2, and 2 (ref. 18). Once again the experimental measurements do not substantiate the ranking of inherent flexibilities; PαMS is much stiffer.

To justify B & W's implicit extension of the G theory to include n, more than a simple static definition of beads and flexes is necessary. For the G–DM expression one approach is to ascribe some of the $\bar{x}$'s to beads and others to flexes. A more general approach, however, is to consider a dynamic lattice model in which the beads occupy the required space but the flexes represent more than a mere accounting of mobile bonding sites. Within this context an inter- as well as an intramolecular flexibility should be considered in order to have a more realistic appraisal of chain mobility. Otherwise, the extreme situations of either inherently stiff molecules with comparatively sessile pseudolattices or flexible ether linkages within fluid-like lattices may be misinterpreted. In an attempt to bridge the gap between these two approaches, the following results first generalize the G theory in terms of n.

RESULTS

The reduced plot of T_g *versus* $\bar{P}^{-1}$ is shown in *Figure 2* as a function of n and V_0. As previously for the G–DM theory, the $T_g/T_{g\infty}$ is evaluated from the point where chain end effects are likely to interfere with the model ($\bar{P} = 10$) to the point where the functions are clearly converging towards the 'infinite' molecular weight polymer, $\bar{P} = 1000$. Similarly the index, n, varies from 0.5 to 25 and includes the original interpretation of G ($\bar{x} = 2\bar{P}$) as well as that of B & W ($\bar{x} = \bar{P}$). Like the G–DM theory, V_0 ranges from 0.015 to 0.045 (*cf.* hatched regions). However, unlike the G–DM theory, the $T_g/T_{g\infty}$ decreases with decreasing V_0* for all n's except $n = 0.5$. In that case as $10^3/\bar{P}$ increases a critical point occurs at $10^3/\bar{P} \approx 70$, in which the upper and lower traces for $V_0 = 0.045$ and $V_0 = 0.015$ (not shown) reverse positions relative to this lowest of the six $V_0 = 0.030$ lines shown. *Table 1* illustrates this V_0 reversal for $n = 0.5$ between $10^3/\bar{P}$ of 50 and 75. Aside from this complication, each of the hatched regions (including the $n = 0.5$ for $10^3/\bar{P} \leqslant 50$) converge upon its respective $V_0 = 0.030$ line as the molecular weight increases. The relative rate at which this occurs can be estimated from the data displayed for $n = 2$ in *Table 2*.

Having considered the general variation of the G theory, the logical extension is to compare the theory with the available experimental data. If analyses are restricted to only those polymers which have at least 25 data points reasonably distributed over a wide range of molecular weight, then only PMMA, polystyrene (PS), poly(vinyl chloride) (PVC), and poly-α-methyl styrene (PαMS) may be considered. When the experimental data of these

* The variation in the major lattice co-ordination number z', over the range 4–12 has been generally discussed by Moacanin and Simha[12] and specifically considered by Eisenberg[13] for sodium phosphate polymers. Moreover, when $\varepsilon \approx 1$ Kcal mol^{-1} segment, the hole energy ($E_0 = z'\alpha/2$ where $z' = 4$)[14] affects β little for $\alpha > 1$ (ref. 15), so that $\alpha = \infty$ (*cf.* Figure 1 and footnote 18 of ref. 4). Further enumeration on both the 'semi-empirical' parameter, ε, and the co-ordination numbers, z and z', may be found in Gordon *et al.*[16]

* The apparent reversal in these normalized plots is a result of the slope changes in the absolute plots (*cf.* Discussion, ref. 11) and not a result of a fundamental difference in the theoretical treatment.

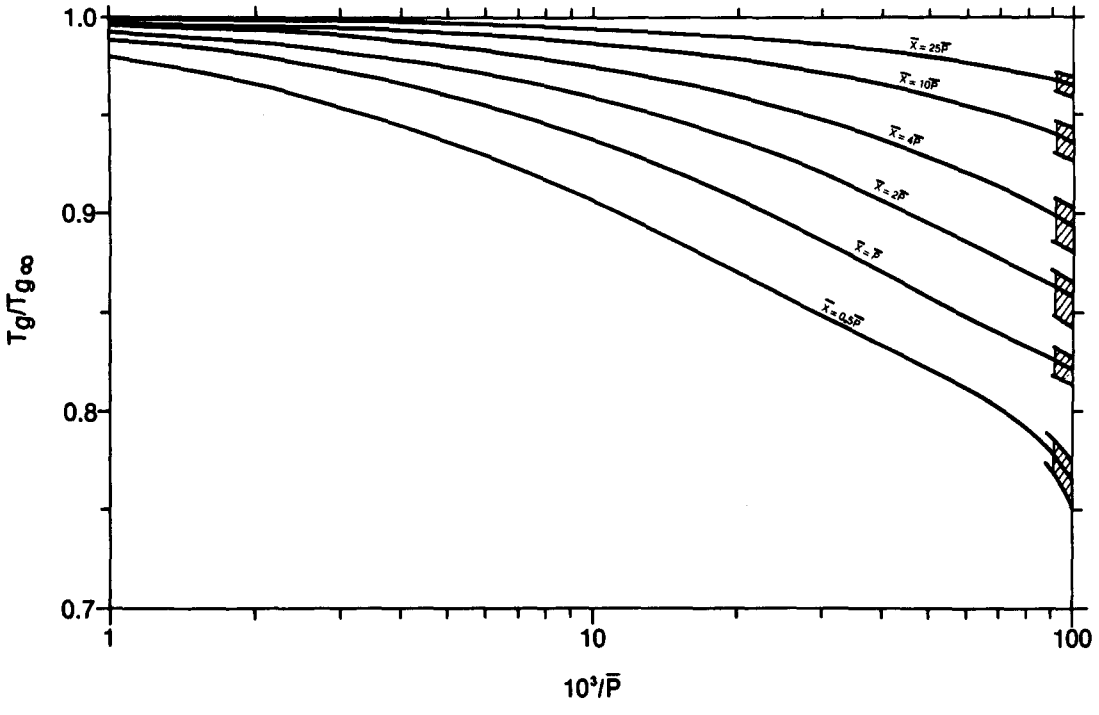

Figure 2 Reduced variables plot indicating the dependence of the glass transition (T_g) upon the logarithmic reciprocal degree of polymerization ($\bar{P}^{-1}$) as a function of free volume fraction ($V_0=0.030$) and number-average of chain atom segments ($\bar{x}$) per $\bar{P}$ ($n=0.5$, 1, 2, 4, 10, and 25). The hatched regions represent the terminus for $V_0=0.015$ and $V_0=0.045$ (*cf.* Results section). These reduced curves assume any constant value of flex energy (ε)

Table 1 $T_g/T_{g\infty}$ values for G theory when $\bar{x} = 0.5\bar{P}$

V_0 \ $10^3/\bar{P}$	10	25	50	75	100
0.045	0.913	0.867	0.825	0.796	0.751
0.030	0.906	0.857	0.822	0.797	0.763
0.015	0.893	0.843	0.813	0.799	0.775

Table 2 $T_g/T_{g\infty}$ values for G theory when $\bar{x} = 2\bar{P}$

V_0 \ $10^3/\bar{P}$	10	25	50	75	100
0.045	0.964	0.936	0.903	0.882	0.866
0.030	0.959	0.928	0.895	0.874	0.859
0.015	0.952	0.915	0.881	0.859	0.843

polymers were compared with the G theory, the statistical analysis methodology which follows eliminated the latter three polymers. (To conserve space these results will not be shown.) Thereby, only eight data sets for PMMA remained: Those prepared by free-radical polymerization (○ and ◒)[1,7] or by radiation degradation (⊗, ●, and ◓)[6,8,19], some acrylic blends (◌)[9], and two stereoregular sets (◑ and ◐)[5]. When these data are plotted using the reduced format, *Figure 3* results. In *Figure 3a* two curves are transcribed from *Figure 2*, one which represents the original G solution ($\bar{x}=2\bar{P}$, upper curve) and another which corresponds to the B & W interpretation ($\bar{x}=\bar{P}$, lower curve). Both curves relate to the early models of an iso-free volume state, $V_0=0.030$. Of the two, $\bar{x}=\bar{P}$ appears to fit the data best. This same fit also looks best when the original G–DM solution ($\bar{x}=2\bar{P}$, $V_0=0.030$) is compared with the B & W solution of the G theory (*cf. Figure 3b*). Other G–DM curves for $\bar{x}=\bar{P}$ and either $r=1.0$ or $V_0=0.030$ do not appear to approximate the data as well (*cf.* Figure 5, ref. 10). The variation of the B & W interpretation of the G theory for $\bar{x}=\bar{P}$, $V_0=0.045$ (upper curve) and $\bar{x}=\bar{P}$, $V_0=0.015$ (lower curve) merely confirmed the observations that V_0 was of lesser importance than n and that the curves were converging for $\bar{P}\rightarrow\infty$ (*cf. Figure 3c*). Once again an inversion of the V_0 parameter would occur for $n=1$ if $\bar{P}$ were less than 10 (*cr. Table 1*).

DISCUSSION

Statistical analysis using the entropic equation of state (equation (1))

By inspection, the initial comparison of the various theoretical approaches to the experimental results leads to a preliminary appraisal of the theory and experiment: that the G theory with $\bar{x}=\bar{P}$ and $V_0=0.030$ is satisfactory (middle curve, *Figure 3c*). Previous experimental analyses have relied on this subjective type of evaluation. It seems reasonable that, as the theoretical approaches increase in sophistication, some objective curve fitting techniques should be advanced. If (at least until a greater number of more accurate T_g measurements are available) all data are weighed equally (regardless of source, synthesis details, tacticity, physical form, thermal history, and test methodology), then a sufficient data base might be obtained which will lend itself to a statistical approach.

The details of the general method are straightforward and involve the use of linear regression techniques[20]. Prerequisites for using this methodology are that the data be normally distributed and homoscedastic, i.e. the variance of the different data sets be equal. A specific solution is sought by first plotting a scatter diagram of the difference between T_r of the theoretical expression and each experimental data point (δ)* *versus* the $\log_{10} 10^3/\bar{P}$.

* Actually, $\delta=[(T_g/T_{g\infty})_{\text{Theoretical}}-(T_g/T_{g\infty})_{\text{Experimental}}]=[(\beta_\infty/\beta)_{\text{Theoretical}}-(\beta_\infty/\beta)_{\text{Experimental}}]$ for any arbitrary but constant ε.

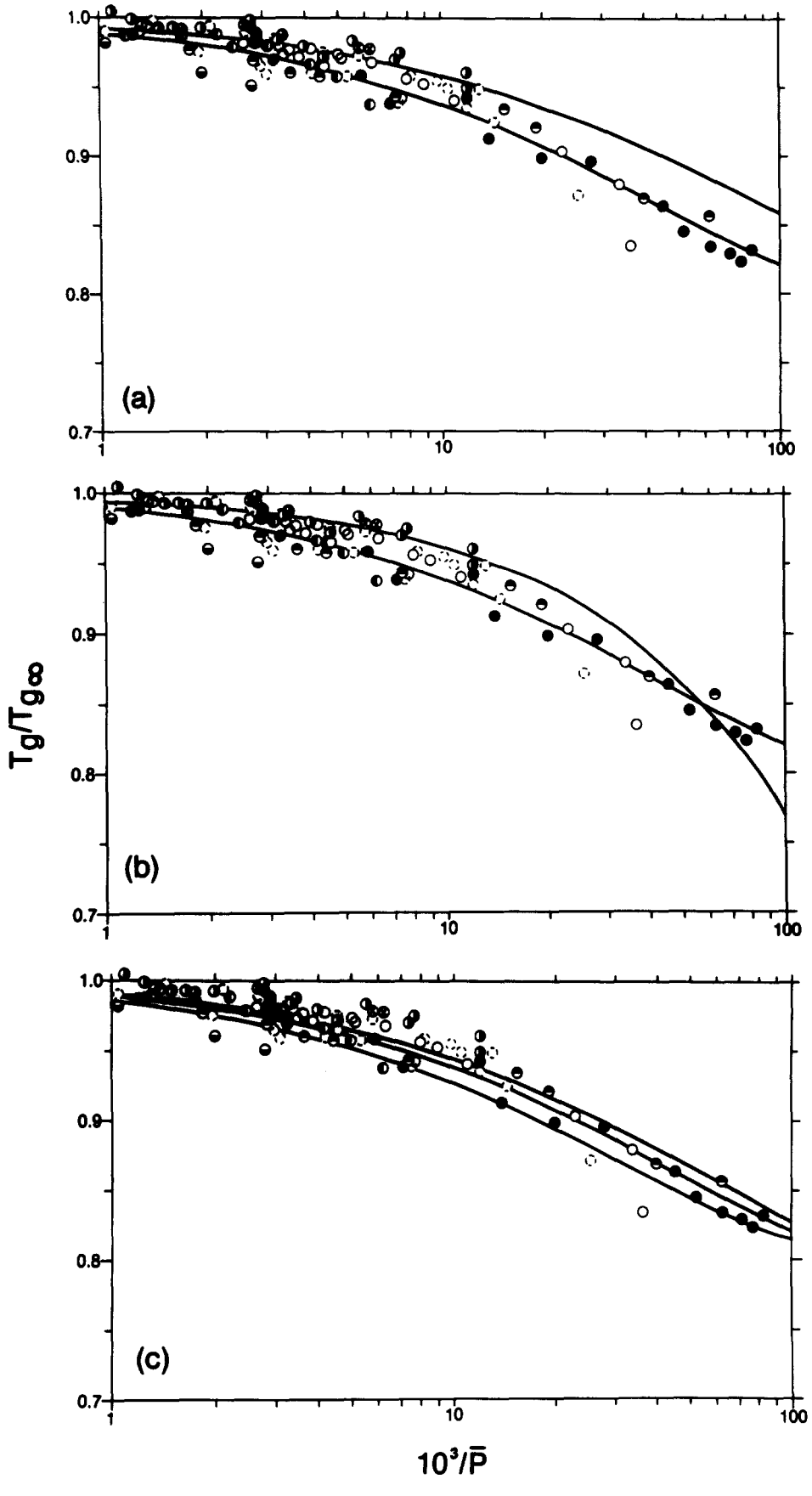

Figure 3 Reduced variables plot for PMMA: ○, Beevers and White[1]; ◒, Kim *et al.*[7]; ◓, Kusy and Greenberg[19]; ●, Kusy *et al.*[8]; ◌, Kusy *et al.* on blends[9]; ⊗, Pratt[6]; ◑, Thompson on isotactic PMMA[5]; and ◐, Thompson on syndiotactic PMMA[5]: (a), curves represent the solution of the G theory for $\bar{x}=2\bar{P}$, $V_0=0.030$ (original interpretation; upper) and for $\bar{x}=\bar{P}$, $V_0=0.030$ (B & W interpretation; lower); (b), curves compare the G–DM theory for $\bar{x}=2\bar{P}$, $V_0=0.030$, and $r=0.9$–1.1 (upper) to the G theory via B & W for $\bar{x}=\bar{P}$, $V_0=0.030$ (lower); and (c), curves illustrate the influence that V_0 has on the G theory when $\bar{x}=\bar{P}$ and $V_0=0.045$ (upper), $V_0=0.030$ (middle), or $V_0=0.015$ (lower)

Use of the logarithmic function is an essential feature of this approach since an otherwise curvilinear relation is transformed to a rectilinear one. A regression line is then drawn through the scatter diagram, and the statistical significance is assessed by means of an F test[21]. If there is no significant difference between theoretical and experimental values (designated the null hypothesis), then both the slope and the intercept of the regression line will not significantly differ from zero. F-values are determined as a function of n (or V_0), given a value of V_0 (or n) and a range of $10^3/\bar{P}$. If $p \leqslant 0.05$, then the nyll hypothesis must be rejected and the alternative hypothesis (i.e. the experimental results and the theoretical predictions are not in agreement) must be adopted.

If for constant V_0 (or n) some values of n (or V_0) are found that satisfy the null hypothesis, then all solution sets of (V_0, n) are plotted for $p = 0.05$. This is accomplished for each satisfactory scatter diagram by transferring to a V_0–n plot those (V_0, n) co-ordinates that correspond to $p = 0.05$ on the F-test plot. The loci of these upper and lower n (or V_0) values for constant V_0 (or n) form an envelope within which $p > 0.05$. Depending upon the exact nature of the data set(s), the inherent scatter of each data set, and the statistical significance associated with p, the (V_0, n) solution set(s) could result in a point or line, but most likely in a closed or open-ended band (e.g. for PMMA) or in the null set, i.e. where no combination of n and V_0 satisfy the criteria (e.g. PS, PVC, and PαMS).

How the analysis proceeds from this juncture depends on the solution set. If a single point results, β^∞ is computed via equation (1) and ε is determined directly provided $T_{g\infty}$ is known (e.g. in refs. 22–24, $T_{g\infty} = 377$ K). If this solution is a line, however, one of two alternatives will apply. If V_0 is a constant the solution for a single point prevails, since β^∞ is independent of n. But if V_0 values with n, then a range of β^∞'s and ε's will result over finite limits. This last situation pertains to either a closed or open-ended band, although in the latter case, the applicability of the solution set will be determined by physical limitations on the magnitude of the variables.

Applications of this methodology to PMMA data and the G theory for n and V_0 is shown in *Figures 4–6*. *Figure 4* shows the scatter diagrams for three representative V_0's ranging from 0.045 (top) to 0.015 (bottom), all at $\bar{x} = \bar{P}$ ($n = 1$). When $1 \leqslant 10^3/\bar{P} \leqslant 100$, the data appear to be best distributed around the regression line for the (V_0, n) co-ordinates (0.045, 1). In this case the slope and intercept are indeed close to zero. While the assumption of normality is increasingly difficult to sustain for $10^3/\bar{P} > 20$, non-normality errors do not preclude the use of the F-test, unless the data is extremely skewed[20].

If the level of significance of the F-test *versus* n is plotted, the degree to which the theory describes the data can be directly interpreted (*cf. Figure 5*). For example, when $1 \leqslant 10^3/\bar{P} \leqslant 100$, the left-hand function for $V_0 = 0.045$. In accordance with the null hypothesis, only those n's whose F values equal or exceed those corresponding to $p = 0.05$ will be rejected. Therefore, only the remaining (V_0, n) solutions which are contiguous to the stippled regions (in this case, $F = 3.12$ for 2 and 120 degrees of freedom) are acceptable. Within the context of *Figure 5* then, the solid circle on the $V_0 = 0.045$ curve represents the scatter diagram of *Figure 4a*; whereas the solid circles on the $V_0 = 0.030$ and $V_0 = 0.015$ curves denote *Figures 4b* and *4c*, respectively. Consistent with the qualitative observation made in *Figure 4*, the statistical significance of the (V_0, n) pairs is greatest for the first case.

By transcribing those co-ordinates for which $p = 0.05$ from a F–n plot, the n–V_0 interrelation may be obtained. *Figure 6* emphasizes one particular solution set for $V_0 = 0.030$ as illustrated in *Figure 5* (*cf.* open circles). As a consequence of many F–n plots, a band results which represents combinations of V_0 and n for which the null hypothesis applies. Generally, the results show that solutions occur over the entire range of V_0 with a lower limit of $n \approx 0.70$. Moreover, by defining n as the number of lattice sites occupied per mer in a dynamic rather than in a static sense, the decreases in V_0 at T_g with decreasing molecular weight may be compensated by increases in n (*cf. Figure 2*). More specifically, *Figure 6* amplifies the dilemma that may have prompted the re-interpretation of the G theory: for $n = 2$, V_0 only equals 0.004–0.007. In the literature V_0 typically ranges from 0.015 to 0.045 (*cf.* the corresponding area of *Figure 6* as detailed in *Table 3*)[1-4,8,12,25-32], with the most frequently quoted values being reported in the range 0.025 to 0.035. Regardless of whether an iso-viscosity or an iso-free volume state exists, such low V_0's (i.e. < 0.010) are not reasonable. When B & W defined $n = 1$, at least a portion of that solution set was within the values which are generally regarded as being plausible. As determined from the present statistical analysis, however, that value of n is no more or less significant than many of the other solutions. (For example, compare the mean coordinates at the so-called 'universal' V_0 of 0.025, i.e. (0.025, 1.25) with the midpoint of the acceptable solution set for $n = 1$, i.e. (0.048, 1.00).) Finally, note that the statistical analysis technique rejects the subjective evaluation which was advanced at the outset of this discussion, i.e. that $\bar{x} = \bar{P}$ ($n = 1$) and $V_0 = 0.030$.

Analysis using two equations of state (EVT and PVT)

The G theory was written at a time when the iso-free volume concept was popular. Thereby, a free volume was assumed or the 'universal' value was assigned, and the value for ε was determined via equation (1). As a consequence, ε was successfully used to compensate for any errors associated either with the selection of a V_0 at T_g or with the utilization of the Flory–Huggins lattice model[16].

The preceding approach was considered for the statistical analysis because it had been exclusively applied in the literature. As a referee noted, however, the G approach fails to explicitly consider the PVT equation of state (i.e. equation (11) of ref. 4 or equation (2.15) of ref. 14*):

$$\ln\left(\frac{V_0^{z'/2-1}}{S_0^{z'/2}}\right) = \frac{z'\alpha S_{\bar{x}}^2}{2kT_g} \tag{2}$$

Here the fraction of holes contiguous to a site, S_0, is defined in terms of the number of vacant sites, n_0, and the number of chains $n_{\bar{x}}$ (each comprising $\bar{x}$ segments):

$$S_0 = \frac{z'n_0}{[(z'-2)\bar{x}+2]n_{\bar{x}} + z'n_0} \tag{3}$$

and the fraction of chemically non-bonded but nearest neighbouring segments to a site:

$$S_{\bar{x}} = 1 - S_0 \tag{4}$$

* The equations in these references assume that $z = z'$.

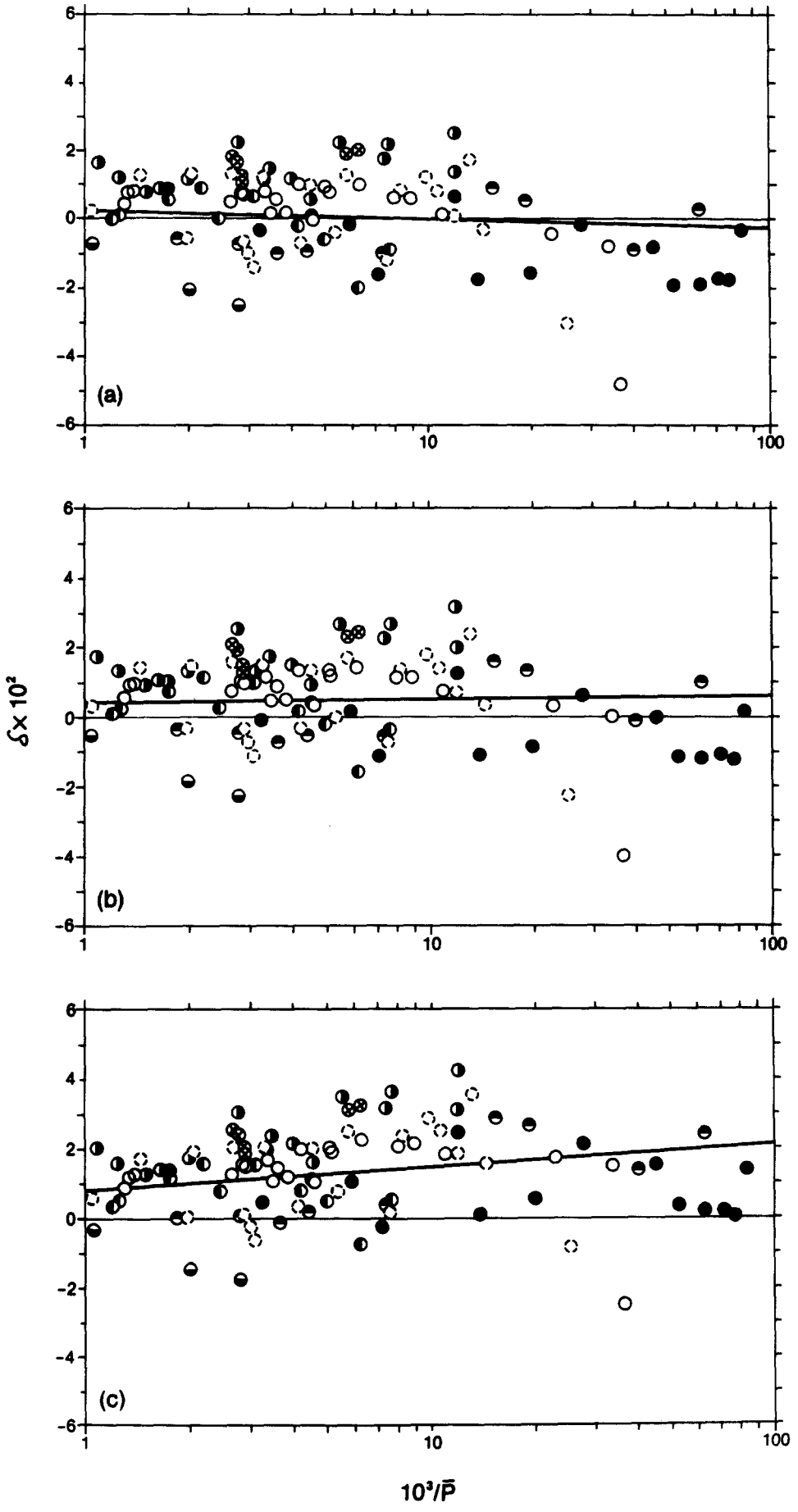

Figure 4 Scatter diagrams for PMMA using G theory in which $\bar{x}=\bar{P}$: (a), $V_0=0.045$; (b), $V_0=0.030$; and (c), $V_0=0.015$ (*cf. Figure 3c*)

Now as the $(\lim)_{z'\to\infty}$, $S_0 = V_0$ and $S_{\bar{x}} = 1 - V_0 = V_{\bar{x}}$. Evaluating equation (2) as $(\lim)_{z'\to\infty}$ and substituting for S_0 and $S_{\bar{x}}$:

$$\beta = -\frac{1}{r}\left[\left(\frac{1-\bar{x}}{\bar{x}(1-V_0)}\right) - \frac{\ln V_0}{(1-V_0)^2}\right] \qquad (5)$$

in which $\beta = -\varepsilon/kT$ and $r = E_0/\varepsilon = z'\alpha/2\varepsilon$. If r is known, a value of V_0 can be found from the recast PVT equation of state (equation (5)), the β and $\bar{x}$ of which satisfy the entropic equation of state (equation (1)). Unfortunately, the value of r is unknown; nevertheless, theoretical curves of V_0 *versus* $T_g/T_{g\infty}$ may be obtained as a function of $\bar{P}$ and r by taking ratios of β_∞/β.

For a given r, *Figure 7* shows that the V_0 dependence with $T_g/T_{g\infty}$ is almost rectilinear over a wide molecular weight range, and that the r curves which may be completely inscribed within the generally accepted V_0 region of 0.015–0.045 (stippled region) range from 1.65 to 2.40. The former observation compares favourably with the specific volume *versus* T_g plot of G–DM in which their theoretical relation (*cf.* Figure 4 of ref. 4) was contrasted against the data of Fox and Flory, and Ueberreiter and Kanig; whereas the latter observation markedly differs from the G–DM theory in which a plot of $-\beta$ *versus* $10^3/\bar{P}$ yielded corresponding r values of 0.93–1.13 (*cf.* Figure 9 of ref. 10).

If a value of $r = 2.0$ were arbitrarily chosen as a point of reference, then over the entire molecular weight range of $10^3/\bar{P} = 0$–100, $T_g/T_{g\infty}$ would decrease 13% while V_0 would decrease by 27%; in the commercial polymer regime ($10^3/\bar{P} < 1$), however, V_0 would decrease only from 0.0318 to 0.0311. Note that, although *Figure 7* was constructed with $n = 1$, the V_0 *versus* $T_g/T_{g\infty}$ plot is valid for any n provided that each $10^3/\bar{P}$ curve is scaled appropriately, i.e. multiplied by n. By using this scaling technique, the case of $n = 2$ may be directly compared with that for $n = 1$. When this is done, both $T_g/T_{g\infty}$ and V_0 decrease to a lesser extent, given the same molecular weight range and the same ratio of hole energy to flex energy considered previously.

If this corresponding range of V_0 (0.024–0.032) is transferred to *Figure 6* along with $n = 2$, the conclusion is immediately obvious: the solution set is outside of the range of statistical significance for PMMA. If this same arbitrary r value is retained over $0 \leqslant 10^3/\bar{P} \leqslant 100$ but n and V_0 are now both varied, then the statistically significant solutions are in a relatively narrow field in which V_0 varies over the range 0.023–0.032 and $n = 1.20 \pm 0.03$ (*cf. Tables 3* and *4* or *Figures 6* and *7*). Of course, another selection of r

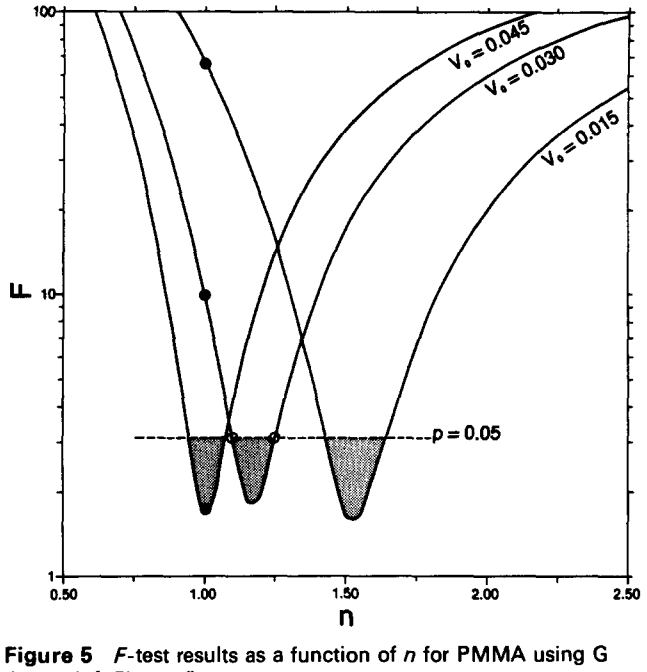

Figure 5 *F*-test results as a function of n for PMMA using G theory (*cf. Figure 4*)

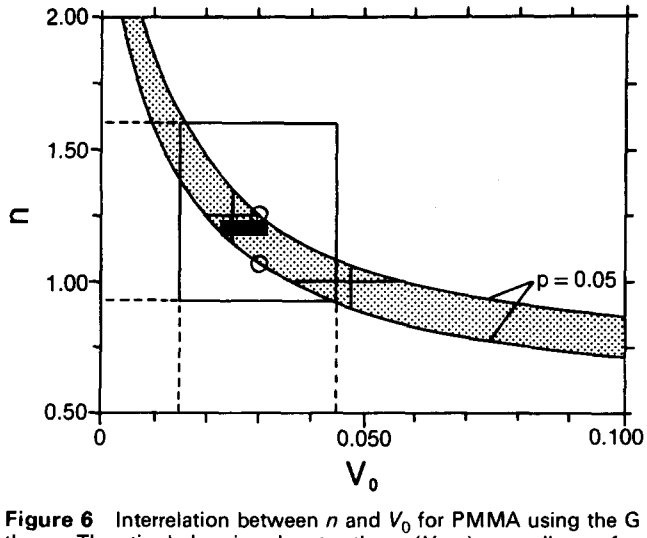

Figure 6 Interrelation between n and V_0 for PMMA using the G theory. The stippled region denotes those (V_0, n) co-ordinates for which the null hypothesis applies. The shaded rectangular field represents the solution set for an arbitrary $r = 2.0$ when $n = 1.20 \pm 0.03$, given a decrease in V_0 from 0.032 to 0.023 as $\bar{P}$ varies from ∞ to 10

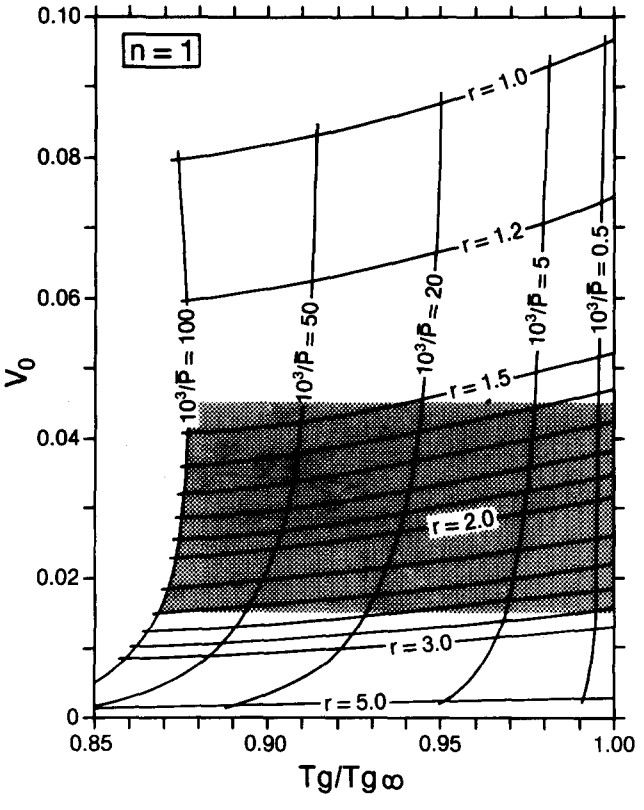

Figure 7 Dependence of V_0 on $T_g/T_{g\infty}$ as a function of $\bar{P}^{-1}$ and inter-/intramolecular energy ratio (r). Although the plot is shown for $n = 1$, the Figure may be scaled for any n simply by multiplying the values for $10^3/\bar{P}$ by n. The stippled region represents $0.015 \leqslant V_0 \leqslant 0.045$

Table 3 *F*-values for selected (V_0, n) co-ordinates and their associated probabilities (PMMA with 2 and 120 degrees of freedom)

n \ V_0	.015	.016	.017	.018	.019	.020	.021	.022	.023	.024	.025	.026	.027	.028	.029	.030	.031	.032	.033	.034	.035	.036	.037	.038	.039	.040	.041	.042	.043	.044	.04
1.50	**1.7**	**1.6**	**1.9**	**2.4**	**3.1**	4.0*	5.0*	6.2*	–	–	10*	–	–	–	–	17*	–	–	–	–	25*	–	–	–	–	32*	–	–	–	–	39*
1.40	4.0*	**2.8**	**2.1**	**1.7**	**1.7**	**1.8**	**2.2**	**2.7**	3.3*	4.1*	5.0*	5.9*	6.9*	–	–	10*	–	–	–	–	16*	–	–	–	–	22*	–	–	–	–	28*
1.30	10*	7.7*	5.8*	4.4*	3.4*	**2.6**	**2.1**	**1.8**	**1.8**	**1.9**	**2.1**	**2.5**	**2.9**	3.5*	4.2*	4.9*	5.6*	6.4*	7.3*	–	9.1*	–	–	–	–	14*	–	–	–	–	19*
1.20	21*	–	–	–	–	7.5*	5.9*	4.6*	3.8*	**3.0**	**2.5**	**2.1**	**1.9**	**1.8**	**1.8**	**2.0**	**2.2**	**2.5**	**2.9**	3.3*	3.8*	4.4*	4.9*	5.5*	6.2*	6.8*	7.5*	8.2*	–	–	10*
1.10	39*	–	–	–	–	18*	–	–	–	9.1*	7.6*	6.4*	5.3*	4.4*	3.6*	**3.0**	**2.6**	**2.3**	**2.0**	**1.9**	**1.8**	**1.8**	**1.9**	**2.0**	**2.2**	**2.4**	**2.7**	**3.0**	3.3*	3.7*	4.
1.00	66*	–	–	–	–	36*	–	–	–	–	19*	–	–	–	–	10*	8.6*	7.7*	6.5*	5.6*	4.9*	4.2*	3.6*	3.3*	**2.8**	**2.5**	**2.2**	**2.0**	**1.9**	**1.7**	1.

* $p \leqslant 0.05$. Therefore, the null hypothesis is acceptable only for those cases which are highlighted in boldface type

Table 4 Free volume (V_0) as a function of the ratio of hole energy to flex energy ($r = E_0/\epsilon = z'\alpha/2\epsilon$) and reciprocal degree of polymerization ($10^3/\bar{P}$)

$10^3/\bar{P}$ \ r	1.4	1.5	1.6	1.7	1.8	1.9	2.0	2.1	2.2	2.3	2.4	2.5	2.6	2.7	2.8	2.9	3.0
10^{-4}	0.059[a]	0.053	0.047	0.043	0.038	0.035	0.032	0.029	0.026	0.024	0.022	0.020	0.019	0.017	0.016	0.015	0.014
1	0.058	0.052	0.047	0.042	0.038	0.034	0.031	0.029	0.026	0.024	0.022	0.020	0.018	0.017	0.016	0.014	0.013
10	0.055	0.049	0.044	0.039	0.036	0.032	0.029	0.026	0.024	0.022	0.020	0.018	0.017	0.015	0.014	0.013	0.012
100	0.047	0.042	0.037	0.033	0.029	0.026	0.024	0.021	0.019	0.017	0.016	0.014	0.013	0.011	0.010	0.009	0.009

[a] Although these V_0 values are specified for $n = 1.50$, they are also accurate (±0.001) for $n = 1.00$–2.00. From an r value's corresponding V_0 range, the permissible (V_0, n) combinations may be determined via the boldface entries of *Table 3*

could yield different but statistically acceptable combinations of (V_0, n). Clearly, more experimental work is needed and a better lattice model than the Meyer–Flory–Huggins is warranted before a more definitive solution can be obtained.

CONCLUSIONS

After a brief description of the reduced T_g parameter plot, the influence of free volume fraction and chain segment density on the G theory of the glass transition has been shown as a function of $\bar{P}^{-1}$. Of the four polymers which have more than 25 T_g data points available, only PMMA satisfied the statistical criteria and required further consideration. Via *subjective* means, the PMMA literature report $n=1$ and $V_0=0.025$ for an $\varepsilon=0.96$–1.00 Kcal mol^{-1} segment, while a current similar analysis estimated that $n=1$ and $V_0=0.030$ for an $\varepsilon=0.98$ Kcal mol^{-1} segment ($T_{g\infty}=377$ K). Using a transformation in regression and an F-test, an *objective* analysis established that many satisfactory (V_0, n) combinations occur, of which (0.048, 1.00) and (0.006, 2.00) are just two. Consequently, a unique solution may only be obtained if in some way a value for V_0 is assumed or if the ratio of hole to flex energy is assigned and the PVT equation of state is solved simultaneously with the EVT equation of state.

ACKNOWLEDGEMENT

The authors with to thank Dr John Karon of the Department of Biostatistics at U.N.C. for his discussions regarding the statistical approach and Dr Edmund DiMarzio of the Polymer Division at the N.B.S. for his discussions regarding the theory.

This investigation was supported by NIH Research Grant No. DE02668 and RCDA No. DE00052 (RPK).

REFERENCES

1 Beevers, R. B. and White, E. F. T. *Trans. Farad. Soc.* 1960, **56**, 744
2 Fox, T. G. and Flory, P. J. *J. Appl. Phys.* 1950, **21**, 581
3 Gibbs, J. H. *J. Chem. Phys.* 1956, **25**, 185
4 Gibbs, J. H. and DiMarzio, E. A. *J. Chem. Phys.* 1958, **28**, 373
5 Thompson, E. V. *J. Polym. Sci.* 1966, **4**, 199
6 Pratt, G. J. *J. Mat. Sci.* 1975, **10**, 809
7 Kim, S. L., Skibo, M., Manson, J. A. and Hertzberg, R. W. *Polym. Eng. Sci.* 1977, **17**, 194
8 Kusy, R. P., Katz, M. J. and Turner, D. T. *Thermochimica Acta* 1978, **26**, 415
9 Kusy, R. P., Simmons, W. F. and Greenberg, A. R. *Polymer* 1981, **22**, 268
10 Greenberg, A. R. and Kusy, R. P. *Polymer* 1983, **24**, 513
11 Kusy, R. P. and Greenberg, A. R. *Polymer* 1982, **23**, 36
12 Moacanin, J. and Simha, R. *J. Chem. Phys.* 1966, **45**, 964
13 Eisenberg, A. 'Advances in Polymer Science', Springer-Verlag, 1967, Vol. 5, p. 59
14 DiMarzio, E. A., Gibbs, J. H., Fleming, P. D. and Sanchez, I. C. *Macromolecules* 1976, **9**, 763
15 DiMarzio, E. A. *Annals N.Y. Acad. Sci.* 1981, **371**, 1
16 Gordon, M., Kapadia, P. and Malakis, A. *J. Phys. A: Math. Gen.* 1976, **9**, 751
17 Wunderlich, B. *J. Phys. Chem.* 1960, **64**, 1052
18 DiMarzio, E. A. and Dowell, F. *J. Appl. Phys.* 1979, **50**, 6061
19 Kusy, R. P. and Greenberg, A. R. *J. Thermal Anal.* 1980, **18**, 117
20 Sokal, R. R. and Rohlf, F. J. 'Biometry', W. H. Freeman, 1969, Ch. 7, 13, and 14
21 Neter, J. and Wasserman, W. 'Applied Linear Statistical Models', R. D. Irwin, Inc., Homewood, Illinois, 1974, Ch. 5
22 Wittmann, J. C. and Kovacs, A. J. *J. Polym. Sci. C* 1969, **16**, 4443
23 Loshaek, S. *J. Polym. Sci.* 1955, **15**, 391
24 Rogers, S. S. and Mandelkern, L. *J. Phys. Chem.* 1957, **61**, 945
25 Williams, M. L., Landel, R. F. and Ferry, J. D. *J. Am. Chem. Soc.* 1955, **77**, 3701
26 Williams, M. L. *J. Appl. Phys.* 1958, **29**, 1395
27 Ferry, J. D. 'Viscoelastic Properties of Polymers', John Wiley, New York, 1961, p. 226
28 Simha, R. and Boyer, R. F. *J. Chem. Phys.* 1962, **37**, 1003
29 Boyer, R. F. *Rubber Chem. Technol.* 1963, **36**, 1303
30 Mason, P. *J. Chem. Phys.* 1964, **35**, 625
31 Miller, A. A. *J. Polym. Sci.* 1964, **A2**, 1095
32 Eisenberg, A. and Saito, S. *J. Chem. Phys.* 1966, **45**, 1673